Mixed finite elements for Kirchhoff–Love plate bending *

Thomas Führer† Norbert Heuer†

Abstract

We present a mixed finite element method with parallelogram meshes for the Kirchhoff–Love plate bending model. Critical ingredient is the construction of appropriate basis functions that are conforming in terms of a sufficiently large tensor space and allow for any kind of physically relevant Dirichlet and Neumann boundary conditions. For Dirichlet boundary conditions, and polygonal convex or non-convex plates that can be discretized by parallelogram meshes, we prove quasi-optimal convergence of the mixed scheme. Numerical results for regular and singular examples with different boundary conditions illustrate our findings.

AMS Subject Classification: 74S05, 35J35, 65N30, 74K20

1 Introduction

Plate bending models have been the subject of research in numerical analysis for several decades, until today. This is not only due to their relevance in structural engineering but also owed to the inherent mathematical challenges. The Kirchhoff–Love and Reissner–Mindlin models are the classical ones. The former can be interpreted as the singularly perturbed limit of the latter for plate thickness tending to zero. This limit case poses the vertical deflection u as an $H^2(\Omega)$-function whereas the bending moments $\boldsymbol{M}$ are set in the space of symmetric $L_2(\Omega)$-tensors with $\operatorname{div}\mathbf{div}\boldsymbol{M} \in L_2(\Omega)$ for L_2-regular vertical loads f, in short, $\boldsymbol{M} \in \mathbb{H}(\operatorname{div}\mathbf{div}, \Omega)$. (Here, $\Omega \subset \mathbb{R}^2$ denotes the plate's mid-surface, and $\mathbf{div}\boldsymbol{M}$ means the row-wise application of the divergence operator.) For non-convex polygonal plates, $\mathbb{H}(\operatorname{div}\mathbf{div}, \Omega)$ is not a subspace of $\mathbb{H}^1(\Omega)$ (tensors with $H^1(\Omega)$-components) or $\mathbb{H}(\mathbf{div}, \Omega)$ (symmetric tensors $\boldsymbol{M}$ with $\mathbf{div}\boldsymbol{M} \in \boldsymbol{L}_2(\Omega) := L_2(\Omega)^2$), cf. [3]. This lack of regularity constitutes a serious challenge for the approximation of bending moments and its analysis. Bending moments are critical quantities in engineering applications and have been elusive to conforming approximations in $\mathbb{H}(\operatorname{div}\mathbf{div}, \Omega)$ for a long time. An early, only partially conforming approach is the Hellan–Herrmann–Johnson method that gives bending moment approximations with continuous normal-normal traces, see [14, 15, 18].

In this paper, we present simple shape functions of lowest degree on parallelograms. They are easy to implement and provide $\mathbb{H}(\operatorname{div}\mathbf{div}, \Omega)$-conformity without requiring any additional non-physical regularity, contrary to other known approaches for triangles, see [6, 17]. Our analysis employs techniques and tools that we have learned from our studies [12, 11] of the discontinuous Petrov–Galerkin (DPG) method in the context of plate bending. Whereas the DPG framework may seem to be very specialized and irrelevant for the analysis of classical Galerkin approaches including mixed schemes, we here illustrate that this view is not correct. The most common DPG setting is based on ultraweak formulations. Their analysis requires a specific formulation of trace operators and the discretization of their images, the resulting trace spaces. On the domain level, these traces give rise to precise conditions of conformity, e.g., across interfaces. For canonical spaces this is well known. For example, $H^1(\Omega)$-conformity requires continuity in

*Supported by ANID through FONDECYT projects 1210391, 1230013

†Facultad de Matemáticas, Pontificia Universidad Católica de Chile, Avenida Vicuña Mackenna 4860, Santiago, Chile, email: {tofuhrer,nheuer}@mat.uc.cl

the sense of $H^{1/2}$-traces and $\boldsymbol{H}(\mathrm{div},\Omega)$-conformity means the $H^{-1/2}$-continuity of normal components. There are spaces where such an approach to conformity is much more intricate, for instance $\mathbb{H}(\mathrm{div}\,\mathbf{div},\Omega)$ introduced before. We stress the fact that there is a key difference between the conformity in the full space and the conformity of piecewise polynomial (or otherwise) approximations. In the latter case, trace operators have to be localized. Considering that trace spaces are typically of fractional order, this is a serious challenge. To circumvent this problem one usually requires more regularity. For instance, normal traces of $\boldsymbol{H}(\mathrm{div},\Omega)$ are considered in L_2 rather than $H^{-1/2}$. The key point is to increase the regularity as little as possible in order not to exclude relevant cases of low regularity. In this paper, we present and analyze a conforming piecewise polynomial approximation of bending moments $\boldsymbol{M}$ which only requires a slightly increased regularity $\boldsymbol{M} \in \mathbb{H}(\mathrm{div}\,\mathbf{div},\Omega,\mathcal{E})$. Here, $\mathbb{H}(\mathrm{div}\,\mathbf{div},\Omega,\mathcal{E}) \subset \mathbb{H}(\mathrm{div}\,\mathbf{div},\Omega)$ is a dense subspace (introduced in §5) and therefore, our construction is applicable without any additional regularity requirement. We use piecewise polynomial tensors on parallelogram meshes. On arbitrary polygonal domains, general quadrilaterals or triangles are needed as well. The construction of corresponding shape functions on such elements is an open problem. Though, for shape functions assuming continuity of bending moments we refer to [6, 7]. Approximations of tensors $\boldsymbol{M} \in \mathbb{H}(\mathbf{div},\Omega) \cap \mathbb{H}(\mathrm{div}\,\mathbf{div},\Omega)$ are studied in [17]. These contributions do not apply to singular cases like plates with non-convex corners we are aiming at, and require more degrees of freedom than necessary for the actual inherent conformity.

We use the trace formulation from [12] to construct $\mathbb{H}(\mathrm{div}\,\mathbf{div},\Omega)$-conforming elements on parallelogram meshes. In contrast to our DPG-setting, where we use lowest-order moments for both the normal-normal traces and the effective shear forces (plus vertex jumps of tangential-normal traces), here we additionally use first-order moments of normal-normal traces. In this way, second-order approximation orders are achieved, in contrast to order one in [12] (though, second order can be easily achieved also in the DPG setting). There is an inherent piecewise polynomial $\mathbb{H}(\mathrm{div}\,\mathbf{div},\Omega)$-interpolation operator. It commutes with the L_2-projection onto piecewise linear polynomials. Therefore, we have the canonical ingredients to set up a mixed finite element scheme and prove second order convergence for sufficiently regular solutions. The vertical deflection is approximated in $L_2(\Omega)$ by piecewise linear polynomials and the bending moments are approximated in $\mathbb{H}(\mathrm{div}\,\mathbf{div},\Omega)$ by our basis functions. We note that an extension of our basis functions to higher approximation orders is open, but not beneficial for the low-regular situation we focus on.

We mention that mixed schemes for Kirchhoff–Love plates have been studied before, see, e.g., [9, 5, 20], to cite a few early papers. They are based on the interpretation of the Kirchhoff–Love model (with isotropic homogeneous material) as the bi-Laplacian, $\Delta^2 u = f$, and introducing $v = \Delta u$ as an independent variable, as proposed by Ciarlet and Raviart in [8]. This strategy requires more regularity than generally available ($v \in H^1(\Omega)$) and does not allow for general Neumann boundary conditions as v is a non-physical variable. We remark that in [10], we presented a DPG-setting for the two-variable setting with $v = \Delta u$ that is well posed for non-convex domains and $L_2(\Omega)$-loads.

The remainder of this paper is as follows. In the next section we introduce some notation, spaces, trace operators, and recall our conformity characterization (Proposition 1). Our new shape functions are defined in Section 3. In Section 4, they are used to construct piecewise polynomial $\mathbb{H}(\mathrm{div}\,\mathbf{div},\Omega)$-conforming approximation spaces. The corresponding interpolation is introduced and analyzed in Section 5, establishing the commutativity and approximation properties (Theorem 8). The mixed formulation and finite element scheme for the Kirchhoff–Love plate being model are presented in Section 6. Theorem 10 establishes the quasi-optimal convergence of the mixed method, with convergence orders for sufficiently smooth solutions given in Corollary 11. Theoretical results in Section 6 are only proved for Dirichlet boundary conditions. Though, we stress the fact that our setting allows for implementing Neumann and mixed boundary conditions as well. Corresponding proofs require more technical details and are left open here. Numerical experiments are reported in Section 7. We present an example with smooth solution on a clamped parallelogram plate, fully covered by our analysis. The second example considers an L-shaped plate with singularity at the incoming corner and mixed boundary conditions. Finally, in Section A, we show samples of the shape functions, one for each of the different categories of degrees of freedom.

Throughout the paper, $a \lesssim b$ means that $a \le cb$ with a generic constant $c > 0$ that is independent of involved functions and the mesh-width parameter h. (We only consider shape-regular parallelogram meshes.) Notation $a \gtrsim b$ means that $b \lesssim a$, and $a \simeq b$ indicates $a \lesssim b$ and $a \gtrsim b$.

2 Spaces and traces

In this section we introduce some canonical Sobolev spaces, and recall tensor spaces and trace operators stemming from the analysis of Kirchhoff–Love plate bending. For details we refer to [12].

For a Lipschitz sub-domain $\omega \subset \mathbb{R}^2$ and non-negative integer m we consider the standard Sobolev spaces $L_2(\omega)$, $H^m(\omega)$, denote the corresponding tensor spaces with blackboard symbols, e.g., $\mathbb{L}_2(\omega) = L_2(\omega)^{2\times 2}$, and define $\mathbb{L}_2^s(\omega) \subset \mathbb{L}_2(\omega)$ as the subspace of symmetric tensors. The corresponding generic norms and seminorms for scalar and tensor-valued functions are $\|\cdot\|_{m,\omega}$ and $|\cdot|_{m,\omega}$, respectively. Throughout, we will drop an index ω when $\omega = \Omega$. On occasion, we employ fractional-order Sobolev spaces $H^{\pm r}(e)$ ($r \in (0,1/2)$) for an edge $e \subset \mathbb{R}^2$ and $\mathbb{H}^r(\omega)$ ($r > 0$) with norm and semi-norm notation as before. For details we refer to [1]. Furthermore, we need the space

$$\mathbb{H}(\mathrm{div}\,\mathbf{div},\omega) := \{\boldsymbol{M} \in \mathbb{L}_2^s(\omega);\ \mathrm{div}\,\mathbf{div}\boldsymbol{M} \in L_2(\omega)\}$$

with canonical graph norm denoted as $\|\cdot\|_{\mathrm{dDiv},\omega}$. Here, $\mathbf{div}\boldsymbol{M}$ is the row-wise calculated divergence of $\boldsymbol{M}$. Following [12] we consider the following trace operators,

$$\mathrm{tr}_\omega^{\mathrm{dDiv}} : \begin{cases} \mathbb{H}(\mathrm{div}\,\mathbf{div},\omega) & \to \quad H^2(\omega)' \\ \quad \boldsymbol{M} & \mapsto \quad \langle \mathrm{tr}_\omega^{\mathrm{dDiv}}(\boldsymbol{M}), z\rangle_{\partial\omega} := (\mathrm{div}\,\mathbf{div}\boldsymbol{M}, z)_\omega - (\boldsymbol{M}, \nabla\nabla z)_\omega, \end{cases} \tag{1}$$

$$\mathrm{tr}_\omega^{\mathrm{Ggrad}} : \begin{cases} H^2(\omega) & \to \quad \mathbb{H}(\mathrm{div}\,\mathbf{div},\omega)' \\ \quad z & \mapsto \quad \langle \mathrm{tr}_\omega^{\mathrm{Ggrad}}(z), \boldsymbol{M}\rangle_{\partial\omega} := \langle \mathrm{tr}_\omega^{\mathrm{dDiv}}(\boldsymbol{M}), z\rangle_{\partial\omega}. \end{cases} \tag{2}$$

Here, $\boldsymbol{\nabla}\boldsymbol{v}$ is the component-wise gradient of a vector function $\boldsymbol{v}$, so that $\boldsymbol{\nabla}\nabla z$ is the Hessian matrix of z. For sufficiently smooth tensor function $\boldsymbol{M}$, scalar function z and boundary $\partial\omega$, traces $\mathrm{tr}_\omega^{\mathrm{dDiv}}(\boldsymbol{M})$ and $\mathrm{tr}_\omega^{\mathrm{Ggrad}}(z)$ reduce to $(\boldsymbol{n}\cdot\boldsymbol{M}\boldsymbol{n})|_{\partial\omega}$, $\big(\boldsymbol{n}\cdot\mathbf{div}\boldsymbol{M} + \partial_{\boldsymbol{t}}(\boldsymbol{t}\cdot\boldsymbol{M}\boldsymbol{n})\big)|_{\partial\omega}$, and $z|_{\partial\omega}$, $(\boldsymbol{n}\cdot\nabla z)|_{\partial\omega}$, respectively. Here, $\boldsymbol{n}$ is the exterior unit normal vector along $\partial\omega$, $\boldsymbol{t}$ is the unit tangential vector along $\partial\omega$ (in mathematically positive orientation), and $\partial_{\boldsymbol{t}}$ denotes the tangential derivative operator. Notation $\boldsymbol{n}$ and $\boldsymbol{t}$ will be generically used for normal and tangential vectors along boundaries of different sub-domains (being defined almost everywhere for polygonal boundaries).

Now, let us consider a conforming mesh $\mathcal{K}$ consisting of shape-regular parallelograms. The sets of edges and interior vertices of $\mathcal{K}$ are $\mathcal{E}$ and $\mathcal{N}_0$, respectively. Correspondingly, the sets of edges and nodes of $K \in \mathcal{K}$ are $\mathcal{E}_K$ and $\mathcal{N}_K$, respectively. Furthermore, for $n \in \mathcal{N}_0$, we will need the subset $\mathcal{K}(n) \subset \mathcal{K}$ of elements that have n as a vertex.

For an element $K \in \mathcal{K}$, an edge $e \in \mathcal{E}_K$ and a smooth symmetric tensor $\boldsymbol{M}$, we denote the edge restrictions of the trace components by

$$\mathrm{tr}_{K,e,\boldsymbol{n}}^{\mathrm{dDiv}}(\boldsymbol{M}) := (\boldsymbol{n}\cdot\boldsymbol{M}\boldsymbol{n})|_e, \quad \mathrm{tr}_{K,e,\boldsymbol{t}}^{\mathrm{dDiv}}(\boldsymbol{M}) := \big(\boldsymbol{n}\cdot\mathbf{div}\boldsymbol{M} + \partial_{\boldsymbol{t}}(\boldsymbol{t}\cdot\boldsymbol{M}\boldsymbol{n})\big)|_e.$$

For bending moments $\boldsymbol{M}$, $\mathrm{tr}_{K,e,\boldsymbol{t}}^{\mathrm{dDiv}}(\boldsymbol{M})$ is the so-called effective shear force on edge e.

In general, there are jumps at the vertices of K,

$$[\boldsymbol{t}\cdot\boldsymbol{M}\boldsymbol{n}]_{\partial K}(n) := (\boldsymbol{t}\cdot\boldsymbol{M}\boldsymbol{n})|_e(x) - (\boldsymbol{t}\cdot\boldsymbol{M}\boldsymbol{n})|_{e'}(n)$$

with $n = \bar{e}\cap\bar{e}' \in \mathcal{N}_K$ being the endpoint of e and starting point of e' for $e, e' \in \mathcal{E}_K$, $e \neq e'$. For an interpretation of the trace components as bounded functionals we need the spaces

$$H^{3/2}(e) := \{z|_e;\ z\in H^2(K)\},\quad H^{1/2}(e) := \{(\boldsymbol{n}\cdot\nabla z)|_e;\ z\in H^2(K)\}\quad (e\in\mathcal{E}_K)$$

with their canonical trace norms. They give rise to the following subspace of $\mathbb{H}(\mathrm{div}\,\mathbf{div}, K)$ (denoted by $\mathcal{H}(\mathrm{div}\,\mathbf{div}, K)$ in [12]),

$$\begin{aligned}&\mathbb{H}(\mathrm{div}\,\mathbf{div}, K, \mathcal{E}_K) :=\\ &\qquad\{\boldsymbol{M}\in\mathbb{H}(\mathrm{div}\,\mathbf{div}, K);\ \mathrm{tr}^{\mathrm{dDiv}}_{K,e,\boldsymbol{n}}(\boldsymbol{M})\in H^{1/2}(e)',\ \mathrm{tr}^{\mathrm{dDiv}}_{K,e,\boldsymbol{t}}(\boldsymbol{M})\in H^{3/2}(e)'\ \forall e\in\mathcal{E}_K\}\end{aligned}$$

endowed with the graph norm. For $\boldsymbol{M}\in\mathbb{H}(\mathrm{div}\,\mathbf{div}, K, \mathcal{E}_K)$, an appropriate weak definition of the jumps $[\boldsymbol{t}\cdot\boldsymbol{M}\boldsymbol{n}]_{\partial K}$ is as a functional acting on the vertex values of $z\in H^2(K)$:

$$[\boldsymbol{t}\cdot\boldsymbol{M}\boldsymbol{n}]_{\partial K}(z) := \sum_{e\in\mathcal{E}_K}\Big(\langle\mathrm{tr}^{\mathrm{dDiv}}_{K,e,\boldsymbol{t}}(\boldsymbol{M}), z\rangle_e - \langle\mathrm{tr}^{\mathrm{dDiv}}_{K,e,\boldsymbol{n}}(\boldsymbol{M}), \boldsymbol{n}\cdot\nabla z\rangle_e\Big) - \langle\mathrm{tr}^{\mathrm{dDiv}}_{K}(\boldsymbol{M}), z\rangle_{\partial K},$$

so that

$$[\boldsymbol{t}\cdot\boldsymbol{M}\boldsymbol{n}]_{\partial K}(n) = [\boldsymbol{t}\cdot\boldsymbol{M}\boldsymbol{n}]_{\partial K}(n)z(n) := [\boldsymbol{t}\cdot\boldsymbol{M}\boldsymbol{n}]_{\partial K}(z) \tag{3}$$

for any $z\in H^2(K)$ with $z(n') = \delta_{n,n'}$ $(n, n'\in\mathcal{N}_K)$, cf. [12, (28), Remark 3.7]. Now, denoting by $\mathbb{H}(\mathrm{div}\,\mathbf{div}, \mathcal{K}, \mathcal{E})$ the product space of $\mathbb{H}(\mathrm{div}\,\mathbf{div}, K, \mathcal{E}_K)$ with respect to mesh $\mathcal{K}$ and identifying $\mathcal{K}$-piecewise defined tensors with the corresponding product elements, we have the following conformity result.

Proposition 1. *A tensor $\boldsymbol{M}\in\mathbb{H}(\mathrm{div}\,\mathbf{div}, \mathcal{K}, \mathcal{E})$ satisfies $\boldsymbol{M}\in\mathbb{H}(\mathrm{div}\,\mathbf{div}, \Omega)$ if and only if*

$$\begin{aligned}&\mathrm{tr}^{\mathrm{dDiv}}_{K_1,e,\boldsymbol{n}}(\boldsymbol{M}) + \mathrm{tr}^{\mathrm{dDiv}}_{K_2,e,\boldsymbol{n}}(\boldsymbol{M}) = 0,\quad \mathrm{tr}^{\mathrm{dDiv}}_{K_1,e,\boldsymbol{t}}(\boldsymbol{M}) + \mathrm{tr}^{\mathrm{dDiv}}_{K_2,e,\boldsymbol{t}}(\boldsymbol{M}) = 0\\ &\qquad\forall e\in\mathcal{E}\ \text{and}\ K_1, K_2\in\mathcal{K}:\ K_1\neq K_2,\ \{e\} = \mathcal{E}_{K_1}\cap\mathcal{E}_{K_2}\\ \text{and}\quad &\sum_{K\in\mathcal{K}(n)}[\boldsymbol{t}\cdot\boldsymbol{M}\boldsymbol{n}]_{\partial K}(n) = 0\ \forall n\in\mathcal{N}_0.\end{aligned}$$

In particular, for $K\in\mathcal{K}$, $e\in\mathcal{E}_K$ and $n\in\mathcal{N}_K$, trace operators $\mathrm{tr}^{\mathrm{dDiv}}_{K,e,\boldsymbol{n}}(\cdot)$, $\mathrm{tr}^{\mathrm{dDiv}}_{K,e,\boldsymbol{t}}(\cdot)$ and jump $[\boldsymbol{t}\cdot(\cdot)\boldsymbol{n}]_{\partial K}(n)$ are bounded linear functionals on $\mathbb{H}(\mathrm{div}\,\mathbf{div}, \mathcal{K}, \mathcal{E})$.

Proof. The conformity characterization is [12, Proposition 3.6]. The well-posedness of the functionals is due to the definition of $\mathbb{H}(\mathrm{div}\,\mathbf{div}, \mathcal{K}, \mathcal{E})$ and standard duality estimates, and is actually used in the proof of the cited proposition. □

3 An $\mathbb{H}(\mathrm{div}\,\mathbf{div})$-element

We consider the reference square $\widehat{K} = (-1, 1)\times(-1, 1)$ with edges and vertices

$$\begin{aligned}&e_1 = (-1,1)\times\{-1\},\quad e_2 = \{1\}\times(-1,1),\quad e_3 = (-1,1)\times\{1\},\quad e_4 = \{-1\}\times(-1,1),\\ &n_1 = (-1,-1),\quad n_2 = (1,-1),\quad n_3 = (1,1),\quad n_4 = (-1,1).\end{aligned}$$

For an interval or line segment I and an open or closed subset $\omega\subset\mathbb{R}^2$, $P^r(I)$ and $\mathcal{P}^r(\omega)$ denote the spaces of polynomials of degree (less than or equal to) r on I and ω, respectively. When there is no ambiguity we will drop the domain arguments of $P^r(I)$ and $\mathcal{P}^r(\omega)$. We use the generic notation $\mathrm{sp}\{\phi_1,\dots\}$ for the space generated by the enclosed scalar or tensor functions $\phi_1,\dots$. Furthermore, for integers $i,j\ge 0$, x^iy^j is understood as the polynomial $(x,y)\mapsto x^iy^j$ with generic domain as needed.

Our discrete space for the reference element is

$$\mathbb{X}^0(\widehat{K}) := \{\boldsymbol{M} = \begin{pmatrix} a & b\\ b & c\end{pmatrix};\ a\in\mathcal{P}^1\oplus\mathrm{sp}\{x^2,x^3\},\ b\in\mathcal{P}^1\oplus\mathrm{sp}\{xy\},\ c\in\mathcal{P}^1\oplus\mathrm{sp}\{y^2,y^3\}\}$$
$$\oplus\,\mathrm{sp}\left\{\begin{pmatrix} xy & \frac{1-y^2}{4}\\ \frac{1-y^2}{4} & 0\end{pmatrix}, \begin{pmatrix} 0 & \frac{1-x^2}{4}\\ \frac{1-x^2}{4} & xy\end{pmatrix}\right\}.$$

The dimension of $\mathbb{X}^0(\widehat{K})$ is 16.

Remark 2. *We note that the last two of the basis functions generating $\mathbb{X}^0(\widehat{K})$ can be represented as*

$$\begin{pmatrix} xy & \frac{1-y^2}{4}\\ \frac{1-y^2}{4} & 0\end{pmatrix} = \frac{1}{2}\,\mathrm{curl}^{\mathrm{s}}\begin{pmatrix} xy^2\\ y\end{pmatrix},\quad \begin{pmatrix} 0 & \frac{1-x^2}{4}\\ \frac{1-x^2}{4} & xy\end{pmatrix} = -\frac{1}{2}\,\mathrm{curl}^{\mathrm{s}}\begin{pmatrix} x\\ x^2y\end{pmatrix}$$

with symmetric curl, $\mathrm{curl}^{\mathrm{s}}\,\boldsymbol{v} := (\mathrm{curl}\,\boldsymbol{v} + (\mathrm{curl}\,\boldsymbol{v})^\top)/2$ *for a vector function* $\boldsymbol{v} = (v_1,v_2)$ *where*

$$\mathrm{curl}\begin{pmatrix} v_1\\ v_2\end{pmatrix} := \begin{pmatrix} \partial_y v_1 & -\partial_x v_1\\ \partial_y v_2 & -\partial_x v_2\end{pmatrix}.$$

It holds $\mathrm{div}\,\mathbf{div}\,\mathrm{curl}^{\mathrm{s}}\,\boldsymbol{v} = 0$ *for any sufficiently smooth vector function* $\boldsymbol{v}$.

In the following, we also need the linear Legendre polynomials $l_j\in P^1(e_j)$ with respect to the arc length in positive orientation, that is, $l_1(x)=x$, $l_2(y)=y$, $l_3(x)=-x$, $l_4(y)=-y$, $-1\le x,y\le 1$. We will establish that $\mathbb{X}^0(\widehat{K})$ has the following degrees of freedom,

$$\mathrm{dof}_j(\boldsymbol{M}) := \langle \mathrm{tr}^{\mathrm{dDiv}}_{\widehat{K},e_j,\boldsymbol{n}}(\boldsymbol{M}), 1\rangle_{e_j},\ \mathrm{dof}_{4+j}(\boldsymbol{M}) := \langle \mathrm{tr}^{\mathrm{dDiv}}_{\widehat{K},e_j,\boldsymbol{n}}(\boldsymbol{M}), l_j\rangle_{e_j}, \tag{4a}$$
$$\mathrm{dof}_{8+j}(\boldsymbol{M}) := \langle \mathrm{tr}^{\mathrm{dDiv}}_{\widehat{K},e_j,\boldsymbol{t}}(\boldsymbol{M}), 1\rangle_{e_j}, \tag{4b}$$
$$\mathrm{dof}_{12+j}(\boldsymbol{M}) := [\boldsymbol{t}\cdot\boldsymbol{M}\boldsymbol{n}]_{\partial\widehat{K}}(n_j) \tag{4c}$$

for $\boldsymbol{M}\in\mathbb{X}^0(\widehat{K})$, $j=1,\dots,4$.

Proposition 3. *Degrees of freedom* (4) *are unisolvent for* $\mathbb{X}^0(\widehat{K})$.

Proof. We first note that $\mathbb{X}^0(\widehat{K})\subset\mathbb{H}(\mathrm{div}\,\mathbf{div},\widehat{K},\mathcal{E}_{\widehat{K}})$ so that degrees of freedom (4) are well defined. To show their one-to-one relation with elements of $\mathbb{X}^0(\widehat{K})$ we simply specify a basis $\{\boldsymbol{\Phi}_i,\ i=1,\dots,16\}$ of tensors so that each of them identifies exactly one of the degrees of freedom, specifically:

$$\begin{aligned}
&\mathrm{dof}_j(\boldsymbol{\Phi}_i) &&= \langle 1,1\rangle_{e_i}\delta_{ij} &&\text{(0th-order moments of normal-normal traces)},\\
&\mathrm{dof}_j(\boldsymbol{\Phi}_{4+i}) &&= \langle l_i,l_i\rangle_{e_i}\delta_{4+i,j} &&\text{(1st-order moments of normal-normal traces)},\\
&\mathrm{dof}_j(\boldsymbol{\Phi}_{8+i}) &&= \langle 1,1\rangle_{e_i}\delta_{8+i,j} &&\text{(0th-order moments of effective shear forces)},\\
&\mathrm{dof}_j(\boldsymbol{\Phi}_{12+i}) &&= \delta_{12+i,j}, &&\text{(jumps of tangential-normal traces)}
\end{aligned}$$

for $j=1,\dots,16$, $i=1,\dots,4$. Of course, $\langle 1,1\rangle_{e_i}=2$ and $\langle l_i,l_i\rangle_{e_i}=2/3$ ($i=1,\dots,4$). The scaling is chosen in such a way that $\mathrm{tr}^{\mathrm{dDiv}}_{\widehat{K},e_i,\boldsymbol{n}}(\boldsymbol{\Phi}_i)=1$, $\mathrm{tr}^{\mathrm{dDiv}}_{\widehat{K},e_i,\boldsymbol{n}}(\boldsymbol{\Phi}_{4+i})=l_i$, and $\mathrm{tr}^{\mathrm{dDiv}}_{\widehat{K},e_i,\boldsymbol{t}}(\boldsymbol{\Phi}_{8+i})=1$ ($i=1,\dots,4$). The corresponding tensors are

$$\boldsymbol{\Phi}_1(x,y) = \frac{1}{8}\begin{pmatrix} 0 & 0\\ 0 & 4-6y+2y^3\end{pmatrix},\quad \boldsymbol{\Phi}_2(x,y) = \frac{1}{8}\begin{pmatrix} 4+6x-2x^3 & 0\\ 0 & 0\end{pmatrix},$$
$$\boldsymbol{\Phi}_3(x,y) = \frac{1}{8}\begin{pmatrix} 0 & 0\\ 0 & 4+6y-2y^3\end{pmatrix},\quad \boldsymbol{\Phi}_4(x,y) = \frac{1}{8}\begin{pmatrix} 4-6x+2x^3 & 0\\ 0 & 0\end{pmatrix},$$

$$\mathbf{\Phi}_5(x,y) = \frac{1}{8}\begin{pmatrix} 0 & x^2-1 \\ x^2-1 & 4x(1-y) \end{pmatrix}, \quad \mathbf{\Phi}_6(x,y) = \frac{1}{8}\begin{pmatrix} 4(1+x)y & 1-y^2 \\ 1-y^2 & 0 \end{pmatrix},$$

$$\mathbf{\Phi}_7(x,y) = \frac{1}{8}\begin{pmatrix} 0 & x^2-1 \\ x^2-1 & -4x(1+y) \end{pmatrix}, \quad \mathbf{\Phi}_8(x,y) = \frac{1}{8}\begin{pmatrix} -4(1-x)y & 1-y^2 \\ 1-y^2 & 0 \end{pmatrix},$$

$$\mathbf{\Phi}_9(x,y) = \frac{1}{4}\begin{pmatrix} 0 & 0 \\ 0 & -1+y+y^2-y^3 \end{pmatrix}, \quad \mathbf{\Phi}_{10}(x,y) = \frac{1}{4}\begin{pmatrix} -1-x+x^2+x^3 & 0 \\ 0 & 0 \end{pmatrix},$$

$$\mathbf{\Phi}_{11}(x,y) = \frac{1}{4}\begin{pmatrix} 0 & 0 \\ 0 & -1-y+y^2+y^3 \end{pmatrix}, \quad \mathbf{\Phi}_{12}(x,y) = \frac{1}{4}\begin{pmatrix} -1+x+x^2-x^3 & 0 \\ 0 & 0 \end{pmatrix},$$

$$\mathbf{\Phi}_{13}(x,y) = \frac{1}{8}\begin{pmatrix} 1-x-x^2+x^3 & 1-x-y+xy \\ 1-x-y+xy & 1-y-y^2+y^3 \end{pmatrix}$$

$$\mathbf{\Phi}_{14}(x,y) = \frac{1}{8}\begin{pmatrix} 1+x-x^2-x^3 & -1-x+y+xy \\ -1-x+y+xy & 1-y-y^2+y^3 \end{pmatrix}$$

$$\mathbf{\Phi}_{15}(x,y) = \frac{1}{8}\begin{pmatrix} 1+x-x^2-x^3 & 1+x+y+xy \\ 1+x+y+xy & 1+y-y^2-y^3 \end{pmatrix}$$

$$\mathbf{\Phi}_{16}(x,y) = \frac{1}{8}\begin{pmatrix} 1-x-x^2+x^3 & -1+x-y+xy \\ -1+x-y+xy & 1+y-y^2-y^3 \end{pmatrix}.$$

For illustration, images of $\mathbf{\Phi}_1$, $\mathbf{\Phi}_5$, $\mathbf{\Phi}_9$, and $\mathbf{\Phi}_{13}$ are shown in Section A. $\square$

We note the following properties of space $\mathbb{X}^0(\widehat{K})$ and its elements.

Lemma 4. *The relations* $\operatorname{div}\mathbf{div}\mathbb{X}^0(\widehat{K}) = \mathcal{P}^1(\widehat{K})$ *and*

$$\operatorname{tr}^{\mathrm{dDiv}}_{\widehat{K},e_j,\boldsymbol{n}}(\boldsymbol{M}) \in P^1(e_j), \quad \operatorname{tr}^{\mathrm{dDiv}}_{\widehat{K},e_j,\boldsymbol{t}}(\boldsymbol{M}) \in P^0(e_j) \quad \forall \boldsymbol{M} \in \mathbb{X}^0(\widehat{K}) \quad (j = 1,\dots,4)$$

hold true.

Proof. The first statement follows by checking that $\operatorname{div}\mathbf{div}\mathbb{X}^0(\widehat{K}) \subset \mathcal{P}^1(\widehat{K})$, and noting that

$$\operatorname{div}\mathbf{div}\mathbf{\Phi}_1 = \frac{3}{2}y, \quad \operatorname{div}\mathbf{div}\mathbf{\Phi}_4 = \frac{3}{2}x, \quad \operatorname{div}\mathbf{div}\mathbf{\Phi}_9 = \frac{1}{2}(1-3y)$$

span $\mathcal{P}^1(\widehat{K})$. The other statements can be seen directly (and were mentioned in the proof of Proposition 3). $\square$

4 A piecewise polynomial $\mathbb{H}(\operatorname{div}\mathbf{div})$-approximation space

To distinguish between objects (functions, tensors, differential operators) related with elements of the mesh and the corresponding ones for reference element $\widehat{K}$, we add the symbol "$\widehat{\ }$" when considering $\widehat{K}$ where needed for clarity. To $K \in \mathcal{K}$ we assign an affine map $F_K: \widehat{K} \to K$,

$$\begin{pmatrix} \widehat{x} \\ \widehat{y} \end{pmatrix} \mapsto \mathbf{B}_K \begin{pmatrix} \widehat{x} \\ \widehat{y} \end{pmatrix} + \boldsymbol{a}_K,$$

where $\boldsymbol{a}_K \in \mathbb{R}^2$, $\mathbf{B}_K \in \mathbb{R}^{2\times 2}$, and set $J_K = \det(\mathbf{B}_K)$. We only consider transformations (thus elements and meshes) which generate families of shape-regular elements, and assume that $|J_K|$ is uniformly bounded.

Tensor functions will be transformed by using the Piola–Kirchhoff transformation to maintain symmetry. For a tensor function $\widehat{\boldsymbol{M}}:\ \widehat{K}\to\mathbb{R}^{2\times 2}$, the transformed function $\boldsymbol{M}:=\mathcal{H}_K(\widehat{\boldsymbol{M}}):\ K\to\mathbb{R}^{2\times 2}$ is defined as

$$|J_K|\boldsymbol{M}\circ F_K := \mathbf{B}_K\widehat{\boldsymbol{M}}\mathbf{B}_K^{\top},$$

cf. [21, Section 3.1] and [11, Section 4.1]. The following lemma collects some properties of transformation $\mathcal{H}_K$.

Lemma 5. *Transformation $\mathcal{H}_K:\ \mathbb{H}(\widehat{\mathrm{div}}\widehat{\mathbf{div}},\widehat{K})\to\mathbb{H}(\mathrm{div}\mathbf{div},K)$ is an isomorphism. For any $\widehat{\boldsymbol{M}}\in\mathbb{H}(\widehat{\mathrm{div}}\widehat{\mathbf{div}},\widehat{K})$ and $\widehat{z}\in H^2(\widehat{K})$, relations*

$$|J_K|(\mathrm{div}\mathbf{div}\boldsymbol{M})\circ F_K=\widehat{\mathrm{div}}\widehat{\mathbf{div}}\widehat{\boldsymbol{M}},\qquad |J_K|(\nabla\nabla z:\boldsymbol{M})\circ F_K=\widehat{\nabla}\widehat{\nabla}\widehat{z}:\widehat{\boldsymbol{M}}$$

hold true with $\boldsymbol{M}=\mathcal{H}_K(\widehat{\boldsymbol{M}})$ and $z=\widehat{z}\circ F_K^{-1}$. Furthermore,

$$\begin{aligned}
&\langle\mathrm{tr}_K^{\mathrm{dDiv}}\boldsymbol{M}\,,z\rangle_{\partial K}=\langle\mathrm{tr}_{\widehat{K}}^{\mathrm{dDiv}}\widehat{\boldsymbol{M}}\,,\widehat{z}\rangle_{\partial\widehat{K}}\quad\forall\boldsymbol{M}\in\mathbb{H}(\mathrm{div}\mathbf{div},K),\ \forall z\in H^2(K),\\
&\left.\begin{array}{l}\|\boldsymbol{M}\|_K\simeq h_K\|\widehat{\boldsymbol{M}}\|_{\widehat{K}}\\ \|\mathrm{div}\mathbf{div}\boldsymbol{M}\|_K\simeq h_K^{-1}\|\widehat{\mathrm{div}}\widehat{\mathbf{div}}\widehat{\boldsymbol{M}}\|_{\widehat{K}}\end{array}\right\}\quad\forall\widehat{\boldsymbol{M}}\in\mathbb{H}(\widehat{\mathrm{div}}\widehat{\mathbf{div}},\widehat{K}).
\end{aligned}$$

Here, the hidden constants are independent of $K\in\mathcal{K}$ and the involved functions.

Proof. We refer to [11, Lemma 8] in the case of triangular elements and note that its proof also applies to parallelograms. □

Using the Piola–Kirchhoff transformation, we define the local spaces and product space

$$\mathbb{X}^0(K):=\mathcal{H}_K(\mathbb{X}^0(\widehat{K})),\quad \mathbb{X}^0(\mathcal{K}):=\Pi_{K\in\mathcal{K}}\mathbb{X}^0(K).$$

Then we define our $\mathbb{H}(\mathrm{div}\mathbf{div},\Omega)$-approximation space as the subspace $\mathbb{X}^{\mathrm{dDiv}}(\mathcal{K})$ of tensors $\boldsymbol{M}=(\boldsymbol{M}_K)_K\in\mathbb{X}^0(\mathcal{K})$ that satisfy

$$\left.\begin{array}{l}\langle\mathrm{tr}_{K,e,\boldsymbol{n}}^{\mathrm{dDiv}}(\boldsymbol{M}_K)+\mathrm{tr}_{K',e,\boldsymbol{n}}^{\mathrm{dDiv}}(\boldsymbol{M}_{K'})\,,l\rangle_e=0\quad\forall l\in P^1(e),\\ \langle\mathrm{tr}_{K,e,\boldsymbol{t}}^{\mathrm{dDiv}}(\boldsymbol{M}_K)+\mathrm{tr}_{K',e,\boldsymbol{t}}^{\mathrm{dDiv}}(\boldsymbol{M}_{K'})\,,1\rangle_e=0\end{array}\right\}\quad\forall K\neq K'\in\mathcal{K}:\ e\in\mathcal{E}_K\cap\mathcal{E}_{K'},\tag{5a}$$

$$\sum_{K\in\mathcal{K}(n)}[\boldsymbol{t}\cdot\boldsymbol{M}_K\boldsymbol{n}]_{\partial K}(n)=0\quad\forall n\in\mathcal{N}_0.\tag{5b}$$

Constraints (5b) are required for tensors $\boldsymbol{M}$ to belong to $\mathbb{H}(\mathrm{div}\mathbf{div},\Omega)$. They can be implemented by representing one of the jumps at $n\in\mathcal{N}_0$ as minus the sum of the others, or by Lagrange multipliers.

Proposition 6. *The inclusion $\mathbb{X}^{\mathrm{dDiv}}(\mathcal{K})\subset\mathbb{H}(\mathrm{div}\mathbf{div},\Omega)$ holds, and the dimension of $\mathbb{X}^{\mathrm{dDiv}}(\mathcal{K})$ is $3\#\mathcal{E}+4\#\mathcal{K}-\#\mathcal{N}_0$. Specifically, every $\boldsymbol{M}\in\mathbb{X}^{\mathrm{dDiv}}(\mathcal{K})$ is uniquely defined by the degrees of freedom*

$$\langle\mathrm{tr}_{K,e,\boldsymbol{n}}^{\mathrm{dDiv}}(\boldsymbol{M})\,,1\rangle_e,\ \langle\mathrm{tr}_{K,e,\boldsymbol{n}}^{\mathrm{dDiv}}(\boldsymbol{M})\,,l_e\rangle_e\quad(e\in\mathcal{E}),\tag{6a}$$

$$\langle\mathrm{tr}_{K,e,\boldsymbol{t}}^{\mathrm{dDiv}}(\boldsymbol{M})\,,1\rangle_e\quad(e\in\mathcal{E}),\tag{6b}$$

$$[\boldsymbol{t}\cdot\boldsymbol{M}|_K\boldsymbol{n}](n)\quad(n\in\mathcal{N}_K,\ K\in\mathcal{K})\tag{6c}$$

$$\textit{subject to}\ \sum_{K\in\mathcal{K}(n)}[\boldsymbol{t}\cdot\boldsymbol{M}|_K\boldsymbol{n}](n)=0\quad\forall n\in\mathcal{N}_0.\tag{6d}$$

Here, l_e is a non-constant polynomial of degree 1 on e. Of course, degrees of freedom associated with interior edges have to be taken for specific orientations (not required for $\langle\mathrm{tr}_{K,e,\boldsymbol{n}}^{\mathrm{dDiv}}(\boldsymbol{M})\,,1\rangle_e=\langle\boldsymbol{n}\cdot\boldsymbol{M}\boldsymbol{n}\,,1\rangle_e$).

Proof. By Proposition 3 and Lemma 5, every local space $\mathbb{X}^0(K)$ ($K\in\mathcal{K}$) can be identified with the degrees of freedom (6a), (6b), (6c) associated with the edges and vertices of K. By Lemma 4 and again Lemma 5, $\mathrm{tr}^{\mathrm{dDiv}}_{K,e,\boldsymbol{n}}(\boldsymbol{M})\in P^1(e)$ and $\mathrm{tr}^{\mathrm{dDiv}}_{K,e,\boldsymbol{t}}(\boldsymbol{M})\in P^0(e)$ for every $\boldsymbol{M}\in\mathbb{X}^0(K)$, $e\in\mathcal{E}_K$, $K\in\mathcal{K}$. Therefore, degrees of freedom (6a), (6b) uniquely determine the traces $\mathrm{tr}^{\mathrm{dDiv}}_{K,e,\boldsymbol{n}}(\boldsymbol{M})$ and $\mathrm{tr}^{\mathrm{dDiv}}_{K,e,\boldsymbol{t}}(\boldsymbol{M})$. The conformity $\mathbb{X}^{\mathrm{dDiv}}(\mathcal{K})\subset\mathbb{H}(\mathrm{div}\mathbf{div},\Omega)$ then follows by the general conformity characterization of Proposition 1. The dimension of $\mathbb{X}^{\mathrm{dDiv}}(\mathcal{K})$ is obtained by counting degrees of freedom (6). $\square$

5 Conforming approximation of $\mathbb{H}(\mathrm{div}\mathbf{div},\Omega)$

Degrees of freedom (6) of space $\mathbb{X}^{\mathrm{dDiv}}(\mathcal{K})$ give rise to an interpolation operator $\Pi^{\mathrm{dDiv}}:\boldsymbol{M}\mapsto\boldsymbol{M}_h\in\mathbb{X}^{\mathrm{dDiv}}(\mathcal{K})$. We first describe the setting on the reference element, and then consider the interpolation in $\mathbb{X}^{\mathrm{dDiv}}(\mathcal{K})$.

5.1 Reference interpolation operator

We define $\widehat{\Pi}^{\mathrm{dDiv}}:\mathbb{H}(\mathrm{div}\mathbf{div},\widehat{K},\mathcal{E}_{\widehat{K}})\to\mathbb{X}^0(\widehat{K})$ by $\widehat{\Pi}^{\mathrm{dDiv}}(\widehat{\boldsymbol{M}}):=\widehat{\boldsymbol{M}}_h$ with

$$
\begin{aligned}
&\langle\mathrm{tr}^{\mathrm{dDiv}}_{\widehat{K},e_j,\boldsymbol{n}}(\widehat{\boldsymbol{M}}-\widehat{\boldsymbol{M}}_h),\hat{l}\rangle_{e_j}=0\quad\forall\hat{l}\in P^1(e_j) && (j=1,\dots,4),\\
&\langle\mathrm{tr}^{\mathrm{dDiv}}_{\widehat{K},e_j,\boldsymbol{t}}(\widehat{\boldsymbol{M}}-\widehat{\boldsymbol{M}}_h),1\rangle_{e_j}=0 && (j=1,\dots,4),\\
&[\boldsymbol{t}\cdot(\widehat{\boldsymbol{M}}-\widehat{\boldsymbol{M}}_h)\boldsymbol{n}]_{\partial\widehat{K}}(n_j)=0 && (j=1,\dots,4),
\end{aligned}
$$

where the notation is as in (4). We also need the L_2-projector $\widehat{\Pi}^1:L_2(\widehat{K})\to\mathcal{P}^1(\widehat{K})$ onto linear polynomials, and the corresponding operator $\Pi^1:L_2(\Omega)\to\mathcal{P}^1(\mathcal{K})$ onto piecewise polynomials.

Lemma 7. *Operator $\widehat{\Pi}^{\mathrm{dDiv}}:\mathbb{H}(\mathrm{div}\mathbf{div},\widehat{K},\mathcal{E}_{\widehat{K}})\to\mathbb{X}^0(\widehat{K})$ is a well-defined projection and satisfies the commutative property*

$$
\widehat{\mathrm{div}}\widehat{\mathbf{div}}\widehat{\Pi}^{\mathrm{dDiv}}\widehat{\boldsymbol{M}}=\widehat{\Pi}^1\widehat{\mathrm{div}}\widehat{\mathbf{div}}\widehat{\boldsymbol{M}}\quad\forall\widehat{\boldsymbol{M}}\in\mathbb{H}(\mathrm{div}\mathbf{div},\widehat{K},\mathcal{E}_{\widehat{K}}).
$$

Proof. By Proposition 1, degrees of freedom (4) constitute a bounded functional $\mathbb{H}(\mathrm{div}\mathbf{div},\widehat{K},\mathcal{E}_{\widehat{K}})\to\mathbb{R}^{16}$. Then, Proposition 3 shows that $\widehat{\Pi}^{\mathrm{dDiv}}$ is well defined.

Now, given $\widehat{\boldsymbol{M}}\in\mathbb{H}(\mathrm{div}\mathbf{div},\widehat{K},\mathcal{E}_{\widehat{K}})$ we denote $\widehat{\boldsymbol{M}}_h:=\widehat{\Pi}^{\mathrm{dDiv}}\widehat{\boldsymbol{M}}$, and use trace operator $\mathrm{tr}^{\mathrm{dDiv}}_{\widehat{K}}$ and relation (3) for jump operator $[\boldsymbol{t}\cdot(\cdot)\boldsymbol{n}]_{\partial\widehat{K}}$, to calculate for $p\in\mathcal{P}^1(\widehat{K})$

$$
\begin{aligned}
(\widehat{\mathrm{div}}\widehat{\mathbf{div}}\widehat{\boldsymbol{M}}_h,\hat{p})_{\widehat{K}}&=\langle\mathrm{tr}^{\mathrm{dDiv}}_{\widehat{K}}(\widehat{\boldsymbol{M}}_h),\hat{p}\rangle_{\partial\widehat{K}}+(\widehat{\boldsymbol{M}}_h,\widehat{\boldsymbol{\varepsilon}}\widehat{\nabla}\hat{p})_{\widehat{K}}\\
&=\sum_{j=1}^4\langle\mathrm{tr}^{\mathrm{dDiv}}_{\widehat{K},e_j,\boldsymbol{t}}(\widehat{\boldsymbol{M}}_h),\hat{p}\rangle_{e_j}-\sum_{j=1}^4\langle\mathrm{tr}^{\mathrm{dDiv}}_{\widehat{K},e_j,\boldsymbol{n}}(\widehat{\boldsymbol{M}}_h),\boldsymbol{n}\cdot\widehat{\nabla}\hat{p}\rangle_{e_j}-\sum_{j=1}^4[\boldsymbol{t}\cdot\widehat{\boldsymbol{M}}_h\boldsymbol{n}]_{\partial\widehat{K}}(n_j)\hat{p}(n_j)\\
&=\sum_{j=1}^4\langle\mathrm{tr}^{\mathrm{dDiv}}_{\widehat{K},e_j,\boldsymbol{t}}(\widehat{\boldsymbol{M}}),\hat{p}\rangle_{e_j}-\sum_{j=1}^4\langle\mathrm{tr}^{\mathrm{dDiv}}_{\widehat{K},e_j,\boldsymbol{n}}(\widehat{\boldsymbol{M}}),\boldsymbol{n}\cdot\widehat{\nabla}\hat{p}\rangle_{e_j}-\sum_{j=1}^4[\boldsymbol{t}\cdot\widehat{\boldsymbol{M}}\boldsymbol{n}]_{\partial\widehat{K}}(n_j)\hat{p}(n_j)\\
&=(\widehat{\mathrm{div}}\widehat{\mathbf{div}}\widehat{\boldsymbol{M}},\hat{p})_{\widehat{K}}.
\end{aligned}
$$

The statement follows by noting that $\widehat{\mathrm{div}}\widehat{\mathbf{div}}\widehat{\boldsymbol{M}}_h\in\mathcal{P}^1(\widehat{K})$ by Lemma 4. $\square$

5.2 Local and global interpolation operators

For any $K\in\mathcal{K}$, we define the local interpolation operator Π^{dDiv}_K by using the Piola–Kirchhoff transformation $\widehat{K}\to K$,

$$
\Pi^{\mathrm{dDiv}}_K:\mathbb{H}(\mathrm{div}\mathbf{div},K,\mathcal{E}_K)\to\mathbb{X}^0(K),\quad\Pi^{\mathrm{dDiv}}_K\boldsymbol{M}:=\mathcal{H}_K(\widehat{\Pi}^{\mathrm{dDiv}}\widehat{\boldsymbol{M}}).
$$

Introducing the space

$$\mathbb{H}(\mathrm{div}\mathbf{div},\Omega,\mathcal{E}) := \mathbb{H}(\mathrm{div}\mathbf{div},\mathcal{K},\mathcal{E}) \cap \mathbb{H}(\mathrm{div}\mathbf{div},\Omega),$$

the global interpolation operator then is

$$\Pi^{\mathrm{dDiv}} : \mathbb{H}(\mathrm{div}\mathbf{div},\Omega,\mathcal{E}) \to \mathbb{X}^0(\mathcal{K}), \quad (\Pi^{\mathrm{dDiv}}\boldsymbol{M})|_K := \Pi_K^{\mathrm{dDiv}}(\boldsymbol{M}|_K) \quad \forall K \in \mathcal{K}.$$

In the following we need the mesh-width function $h_{\mathcal{K}}|_K := h_K$ ($K \in \mathcal{K}$) where h_K is the diameter of K, and set $h := \max\{h_K;\ K \in \mathcal{K}\}$.

Theorem 8. *Operator Π^{dDiv} is a projection onto $\mathbb{X}^{\mathrm{dDiv}}(\mathcal{K})$, and satisfies*

$$\mathrm{div}\mathbf{div}\Pi^{\mathrm{dDiv}}(\boldsymbol{M}) = \Pi^1 \mathrm{div}\mathbf{div}\boldsymbol{M} \quad \forall \boldsymbol{M} \in \mathbb{H}(\mathrm{div}\mathbf{div},\Omega,\mathcal{E}).$$

Furthermore, for $r > 1$, error estimate

$$\|\boldsymbol{M} - \Pi^{\mathrm{dDiv}}\boldsymbol{M}\| \lesssim h^{\min\{r,2\}}\|\boldsymbol{M}\|_r \quad \forall \boldsymbol{M} \in \mathbb{H}^r(\Omega) \cap \mathbb{L}_2^s(\Omega)$$

holds true. In particular, $\Pi^{\mathrm{dDiv}} : \mathbb{H}^r(\Omega) \cap \mathbb{L}_2^s(\Omega) \to \mathbb{L}_2^s(\Omega)$ is bounded for any $r > 1$.

Proof. The fact that Π^{dDiv} is well defined is due to the definition via Piola–Kirchhoff transformation and reference interpolation operator $\widehat{\Pi}^{\mathrm{dDiv}}$, and an application of Lemma 7. The fact that property $\boldsymbol{M}_h = (\boldsymbol{M}_{h,K})_K := \Pi^{\mathrm{dDiv}}(\boldsymbol{M}) \in \mathbb{X}^{\mathrm{dDiv}}(\mathcal{K})$ for $\boldsymbol{M} = (\boldsymbol{M}_K)_K \in \mathbb{H}(\mathrm{div}\mathbf{div},\Omega,\mathcal{E})$ holds can be seen as follows. Relation (5a) holds by construction since the Piola–Kirchhoff transformation conserves traces by Lemma 5. To establish relation (5b), let $n \in \mathcal{N}_0$ be given. Then,

$$\sum_{K\in\mathcal{K}(n)} [\boldsymbol{t}\cdot\boldsymbol{M}_{h,K}\boldsymbol{n}]_{\partial K}(n) = \sum_{K\in\mathcal{K}(n)} [\boldsymbol{t}\cdot\boldsymbol{M}_K\boldsymbol{n}]_{\partial K}(n) = 0.$$

The first equation is due to construction and the second holds by Proposition 1.

The commutative property is due to a piecewise application of Lemma 7 and transformation properties given by Lemma 5. Specifically, for $p \in \mathcal{P}^1(K)$ and $K \in \mathcal{K}$, we calculate

$$\begin{aligned}(\mathrm{div}\mathbf{div}\Pi_K^{\mathrm{dDiv}}(\boldsymbol{M}), p)_K &= (\mathrm{div}\mathbf{div}\mathcal{H}_K(\widehat{\Pi}^{\mathrm{dDiv}}\widehat{\boldsymbol{M}}), p)_K = (\widehat{\mathrm{div}}\widehat{\mathbf{div}}\widehat{\Pi}^{\mathrm{dDiv}}\widehat{\boldsymbol{M}}, \hat{p})_{\widehat{K}} \\ &= (\widehat{\mathrm{div}}\widehat{\mathbf{div}}\widehat{\boldsymbol{M}}, \hat{p})_{\widehat{K}} = (\mathrm{div}\mathbf{div}\boldsymbol{M}, p)_K \quad \forall \boldsymbol{M} \in \mathbb{H}(\mathrm{div}\mathbf{div}, K, \mathcal{E}_K),\end{aligned}$$

and the commutative property follows by property $\mathrm{div}\mathbf{div}\Pi^{\mathrm{dDiv}}(\boldsymbol{M}) \in \mathcal{P}^1(\mathcal{K})$, cf. Lemma 4.

The last estimate can be shown by canonical arguments, once boundedness of $\widehat{\Pi}^{\mathrm{dDiv}} : \mathbb{H}^r(\widehat{K}) \cap \mathbb{L}_2^s(\widehat{K}) \to \mathbb{L}_2^s(\widehat{K})$ is established. Let us check the boundedness. Given $\widehat{\boldsymbol{M}} \in \mathbb{H}^r(\widehat{K})$ with $r > 1$, $\widehat{\boldsymbol{M}}\boldsymbol{n}|_{\partial\widehat{K}} \in \boldsymbol{L}_2(\partial\widehat{K})$ (vector-valued L_2-functions on $\partial\widehat{K}$) and $\|\widehat{\boldsymbol{M}}\|_{L_\infty(\widehat{K})} \lesssim \|\widehat{\boldsymbol{M}}\|_{r,\widehat{K}}$ by the trace and Sobolev embedding theorems. Furthermore, e being an edge of $\widehat{K}$, $\langle\partial_{\boldsymbol{t}}(\boldsymbol{t}\cdot\widehat{\boldsymbol{M}}\boldsymbol{n}), 1\rangle_e$ is the difference of the values of $\boldsymbol{t}\cdot\widehat{\boldsymbol{M}}\boldsymbol{n}$ at the endpoints of e and thus, bounded as well. Finally, we bound

$$|\langle\boldsymbol{n}\cdot\widehat{\mathbf{div}}\widehat{\boldsymbol{M}}, 1\rangle_e| \lesssim \|\boldsymbol{n}\cdot\widehat{\mathbf{div}}\widehat{\boldsymbol{M}}\|_{r-3/2,e}$$

by using the $H^{r-3/2}(e) \times H^{3/2-r}(e)$ duality for $r \in (1, 3/2)$, cf., e.g., [19]. Then,

$$\|\boldsymbol{n}\cdot\widehat{\mathbf{div}}\widehat{\boldsymbol{M}}\|_{r-3/2,e} \lesssim \|\widehat{\mathrm{div}}\widehat{\mathbf{div}}\widehat{\boldsymbol{M}}\|_{\widehat{K}} + \|\widehat{\mathbf{div}}\widehat{\boldsymbol{M}}\|_{r-1,\widehat{K}} \lesssim \|\widehat{\mathrm{div}}\widehat{\mathbf{div}}\widehat{\boldsymbol{M}}\|_{\widehat{K}} + \|\widehat{\boldsymbol{M}}\|_{r,\widehat{K}}$$

holds by [2, Lemma 2.1]. We have thus verified the boundedness of $\widehat{\Pi}^{\mathrm{dDiv}}$.

The error estimate then follows by local arguments. Specifically, by construction, polynomial tensors of $\mathcal{P}^1(\widehat{K})^{2\times 2} \cap \mathbb{L}_2^s(\widehat{K})$ are being reproduced by $\widehat{\Pi}^{\mathrm{dDiv}}$. Therefore, using the transformation properties established by Lemma 5, the boundedness of $\widehat{\Pi}^{\mathrm{dDiv}}$, the Bramble–Hilbert lemma and scaling properties of semi-norms (cf. [16]), we conclude for $r \in (1, 2]$ that

$$\|\boldsymbol{M} - \Pi^{\mathrm{dDiv}}\boldsymbol{M}\|_K^2 \simeq h_K^2\|\widehat{\boldsymbol{M}} - \widehat{\Pi}^{\mathrm{dDiv}}\widehat{\boldsymbol{M}}\|_{\widehat{K}}^2 \lesssim h_K^2|\widehat{\boldsymbol{M}}|_{\widehat{K},r}^2 \simeq h_K^{2r}|\boldsymbol{M}|_{r,K}^2$$

for any $\boldsymbol{M} \in \mathbb{H}^r(K)$ and $K \in \mathcal{K}$. Summation over $K \in \mathcal{K}$ shows the final statement. □

6 An application to plate bending

Let $\Omega \subset \mathbb{R}^2$ be a simply-connected bounded Lipschitz domain with boundary $\Gamma = \partial\Omega$. For the analysis of our mixed finite element formulation we will assume that Ω is a polygon that can be decomposed into parallelograms. As in [12] we consider the following scaled version of the Kirchhoff–Love plate bending model,

$$\operatorname{div}\mathbf{div}\boldsymbol{M} = f,\ \boldsymbol{M} = \mathcal{C}\nabla\nabla u \text{ in } \Omega, \tag{7}$$

plus boundary conditions. Here, u is the vertical deflection of a thin plate with mid-surface Ω, $\boldsymbol{M}$ are the bending moments, and f represents a (scaled) vertical load. There is a fourth-order tensor $\mathcal{C}$ of material properties, and we assume that $\mathcal{C}:\ \mathbb{L}_2^s(\Omega) \to \mathbb{L}_2^s(\Omega)$ induces a positive definite isomorphism. In particular, its inverse, compliance tensor $\mathcal{C}^{-1}$, is a positive definite isomorphism $\mathbb{L}_2^s(\Omega) \to \mathbb{L}_2^s(\Omega)$.

For simplicity we consider Dirichlet boundary conditions. Boundary data stem from the trace space

$$H^{3/2,1/2}(\Gamma) \coloneqq \operatorname{tr}_\Omega^{\mathrm{Ggrad}}(H^2(\Omega))$$

with respective induced trace norm $\|\cdot\|_{3/2,1/2,\Gamma}$. We also introduce $H_0^2(\Omega)$ as the subspace of $H^2(\Omega)$-functions z with vanishing traces $\operatorname{tr}_\Omega^{\mathrm{Ggrad}}(z)$, the canonical space.

With this preparation at hand, the mixed formulation of Kirchhoff–Love plate bending problem (7) with Dirichlet boundary condition reads as follows. *For given $f \in L_2(\Omega)$ and $\boldsymbol{g} \in H^{3/2,1/2}(\Gamma)$ find $\boldsymbol{M} \in \mathbb{H}(\operatorname{div}\mathbf{div},\Omega)$ and $u \in L_2(\Omega)$ such that*

$$(\mathcal{C}^{-1}\boldsymbol{M}\,,\boldsymbol{\delta}\mathbf{M}) - (u\,,\operatorname{div}\mathbf{div}\boldsymbol{\delta}\mathbf{M}) = -\langle \operatorname{tr}_\Omega^{\mathrm{dDiv}}(\boldsymbol{\delta}\mathbf{M})\,,\boldsymbol{g}\rangle_{\partial\Omega} \quad \forall \boldsymbol{\delta}\mathbf{M} \in \mathbb{H}(\operatorname{div}\mathbf{div},\Omega), \tag{8a}$$

$$(\operatorname{div}\mathbf{div}\boldsymbol{M}\,,\delta u) = (f\,,\delta u) \quad \forall \delta u \in L_2(\Omega). \tag{8b}$$

Proposition 9. *Problem (8) is well posed with unique solution $(u,\boldsymbol{M}) = (u,\mathcal{C}\nabla\nabla u) \in H^2(\Omega) \times \mathbb{H}(\operatorname{div}\mathbf{div},\Omega)$ that satisfies $\operatorname{tr}_\Omega^{\mathrm{Ggrad}}(u) = \boldsymbol{g}$. It is bounded as*

$$\|u\|_2 + \|\boldsymbol{M}\|_{\mathrm{dDiv}} \lesssim \|f\| + \|\boldsymbol{g}\|_{3/2,1/2,\Gamma}.$$

Proof. The statement follows by standard arguments from the Babuška–Brezzi theory, cf., e.g., [4, 13]. Let us briefly comment on them. The right-hand side linear forms are bounded by the definition of trace dualities, the Cauchy–Schwarz inequality and the choice of norms. Given $\boldsymbol{M} \in \mathbb{H}(\operatorname{div}\mathbf{div},\Omega)$ with $(\operatorname{div}\mathbf{div}\boldsymbol{M}\,,\delta u) = 0\ \forall \delta u \in L_2(\Omega)$ it follows that $\operatorname{div}\mathbf{div}\boldsymbol{M} = 0$ so that coercivity $(\mathcal{C}^{-1}\boldsymbol{M}\,,\boldsymbol{M}) \simeq \|\boldsymbol{M}\|_{\mathrm{dDiv}}^2$ holds by the property of $\mathcal{C}$. It only remains to note the surjectivity of

$$\operatorname{div}\mathbf{div}:\ \mathbb{H}(\operatorname{div}\mathbf{div},\Omega) \to L_2(\Omega).$$

In fact, given $f \in L_2(\Omega)$, we define $\boldsymbol{M} \coloneqq \nabla\nabla z$ where $z \in H_0^2(\Omega)$ solves $\Delta^2 z = f$, cf. [3]. It follows that $\boldsymbol{M} \in \mathbb{L}_2^s(\Omega)$ and $\operatorname{div}\mathbf{div}\boldsymbol{M} = f$ as wanted. □

Now, for a discretization of (8), we consider a polygonal domain Ω (composed of parallelograms) and a conforming shape-regular parallelogram mesh $\mathcal{K}$ as introduced in Section 2. Furthermore, let $\mathcal{P}^1(\mathcal{K})$ be the space of piecewise linear polynomials and let $\mathbb{X}^{\mathrm{dDiv}}(\mathcal{K})$ be the $\mathbb{H}(\operatorname{div}\mathbf{div},\Omega)$-conforming approximation space as introduced in §5. The mixed finite element scheme reads as follows. *Find $\boldsymbol{M}_h \in \mathbb{X}^{\mathrm{dDiv}}(\mathcal{K})$ and $u_h \in \mathcal{P}^1(\mathcal{K})$ such that*

$$(\mathcal{C}^{-1}\boldsymbol{M}_h\,,\boldsymbol{\delta}\mathbf{M}) - (u_h\,,\operatorname{div}\mathbf{div}\boldsymbol{\delta}\mathbf{M}) = -\langle \operatorname{tr}_\Omega^{\mathrm{dDiv}}(\boldsymbol{\delta}\mathbf{M})\,,\boldsymbol{g}\rangle_{\partial\Omega} \quad \forall \boldsymbol{\delta}\mathbf{M} \in \mathbb{X}^{\mathrm{dDiv}}(\mathcal{K}), \tag{9a}$$

$$(\operatorname{div}\mathbf{div}\boldsymbol{M}_h\,,\delta u) = (f\,,\delta u) \quad \forall \delta u \in \mathcal{P}^1(\mathcal{K}). \tag{9b}$$

Theorem 10. *For given $f \in L_2(\Omega)$ and $\boldsymbol{g} \in H^{3/2,1/2}(\Gamma)$, let $(u, \boldsymbol{M}) \in H^2(\Omega) \times \mathbb{H}(\mathrm{div}\,\mathbf{div}, \Omega)$ be the solution of* (8)*. Scheme* (9) *has a unique solution $(\boldsymbol{M}_h, u_h)$. It satisfies*

$$\|\boldsymbol{M} - \boldsymbol{M}_h\|_{\mathrm{dDiv}} \lesssim \inf\{\|\boldsymbol{M} - \boldsymbol{Q}\|_{\mathrm{dDiv}};\ \boldsymbol{Q} \in \mathbb{X}^{\mathrm{dDiv}}(\mathcal{K})\}$$

and

$$\|u - u_h\| \lesssim \inf\{\|\boldsymbol{M} - \boldsymbol{Q}\|_{\mathrm{dDiv}};\ \boldsymbol{Q} \in \mathbb{X}^{\mathrm{dDiv}}(\mathcal{K})\} + \inf\{\|u - w\|;\ w \in \mathcal{P}^1(\mathcal{K})\}.$$

Proof. The statement follows by verifying the standard conditions for mixed schemes, see, e.g., [4, 13]. The bilinear and linear forms in (9) are uniformly bounded. The inf-sup property can be seen as follows. Given $u \in \mathcal{P}^1(\mathcal{K})$, we define $z \in H^1_0(\Omega)$ as the solution to $\Delta z = u$ in Ω. Denoting by $\boldsymbol{I}$ the identity tensor, it follows that there is $r > 1$ such that $z\boldsymbol{I} \in \mathbb{H}^r(\Omega) \cap \mathbb{H}(\mathrm{div}\,\mathbf{div}, \Omega)$ and $\boldsymbol{M} := \Pi^{\mathrm{dDiv}}(z\boldsymbol{I})$ is well defined. Furthermore, by Theorem 8, $\mathrm{div}\,\mathbf{div}\boldsymbol{M} = \Pi^1 \mathrm{div}\,\mathbf{div}(z\boldsymbol{I}) = \Pi^1 u = u$ and $\|\boldsymbol{M}\| \lesssim \|z\boldsymbol{I}\|_r \lesssim \|u\|$. Therefore,

$$(\mathrm{div}\,\mathbf{div}\boldsymbol{M}, u) = \|u\|^2 \gtrsim \|\boldsymbol{M}\|_{\mathrm{dDiv}}\|u\|,$$

that is, the discrete inf-sup condition holds with a constant independent of h. The $\mathbb{H}(\mathrm{div}\,\mathbf{div}, \Omega)$-coercivity of bilinear form $(\mathcal{C}^{-1}\cdot, \cdot)$ on

$$\{\boldsymbol{M} \in \mathbb{X}^{\mathrm{dDiv}}(\mathcal{K});\ (\mathrm{div}\,\mathbf{div}\boldsymbol{M}, u) = 0\ \forall u \in \mathcal{P}^1(\mathcal{K})\} = \{\boldsymbol{M} \in \mathbb{X}^{\mathrm{dDiv}}(\mathcal{K});\ \mathrm{div}\,\mathbf{div}\boldsymbol{M} = 0\} \tag{10}$$

holds due to the inclusion $\mathrm{div}\,\mathbf{div}\mathbb{X}^{\mathrm{dDiv}}(\mathcal{K}) \subset \mathcal{P}^1(\mathcal{K})$ and the positive-definiteness of $\mathcal{C}^{-1}$. The quasi-optimal error estimate for $\|\boldsymbol{M} - \boldsymbol{M}_h\|_{\mathrm{dDiv}}$ is due to kernel relation (10). □

As a consequence of the well-posedness of scheme (9) and the approximation properties of Π^{dDiv} by Theorem 8, Theorem 10 gives the following error estimate.

Corollary 11. *For given $f \in L_2(\Omega)$ and $\boldsymbol{g} \in H^{3/2,1/2}(\Gamma)$, let $u \in H^2(\Omega)$ be the solution of* (7) *with $\mathrm{tr}^{\mathrm{Ggrad}}_{\Omega}(u) = \boldsymbol{g}$. Furthermore, let $(\boldsymbol{M}_h, u_h)$ be the solution of* (9)*. If there is $r > 1$ such that $u \in H^{2+r}(\Omega)$, then*

$$\|u - u_h\| + \|\mathcal{C}\nabla\nabla - \boldsymbol{M}_h\|_{\mathrm{dDiv}} \lesssim h^{\min\{r,2\}}\|u\|_{2+r} + \inf_{p \in \mathcal{P}^1(\mathcal{K})} \|f - p\|.$$

7 Numerical experiments

We report on numerical results for a case with smooth solution (Example 1), and a case with singular solution (Example 2). Throughout we use uniform meshes.

Example 1.

Parallelogram domain Ω (figure on the right), exact solution:

$$u(x, y) = (x^2 - 1)^2((x - y)^2 - 1)^2,$$

boundary conditions: $u = \partial_{\boldsymbol{n}} u = 0$ on $\partial\Omega$.

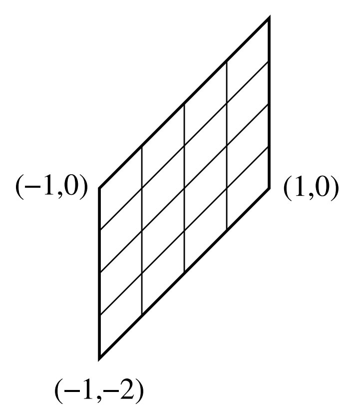

In this case the domain requires a mesh of non-rectangular parallelograms, as shown in the figure. The exact solution is a polynomial with homogeneous trace and normal derivative on the boundary. This case is fully covered by Theorem 10 and Corollary 11. Figure 1 shows the approximation on a mesh with 256 elements, u_h at the top left (indicated by u), and the three components of $\boldsymbol{M}_h$ in the bottom row (indicated by m_{11}, m_{12}, m_{22}). For illustration we also calculate the piecewise divergence of $\boldsymbol{M}_h$, $\mathbf{div}_h \boldsymbol{M}_h$, as an approximation of the shear force $\mathbf{div}\boldsymbol{M}$. It is shown in the top row indicated by q_1, q_2. The L_2-errors $\|u - u_h\|$, $\|\boldsymbol{M} - \boldsymbol{M}_h\|$, $\|\mathrm{div}\,\mathbf{div}(\boldsymbol{M} - \boldsymbol{M}_h)\|$ are plotted in Figure 2 along with a curve $O(h^2) = O(N^{-1})$ ($N := \#\mathcal{K}$) and confirm convergence of order $O(h^2)$. Again for illustration, also the results for $\|\mathbf{div}(\boldsymbol{M} - \boldsymbol{M}_h)\|$ are given and indicate convergence of order $O(h)$.

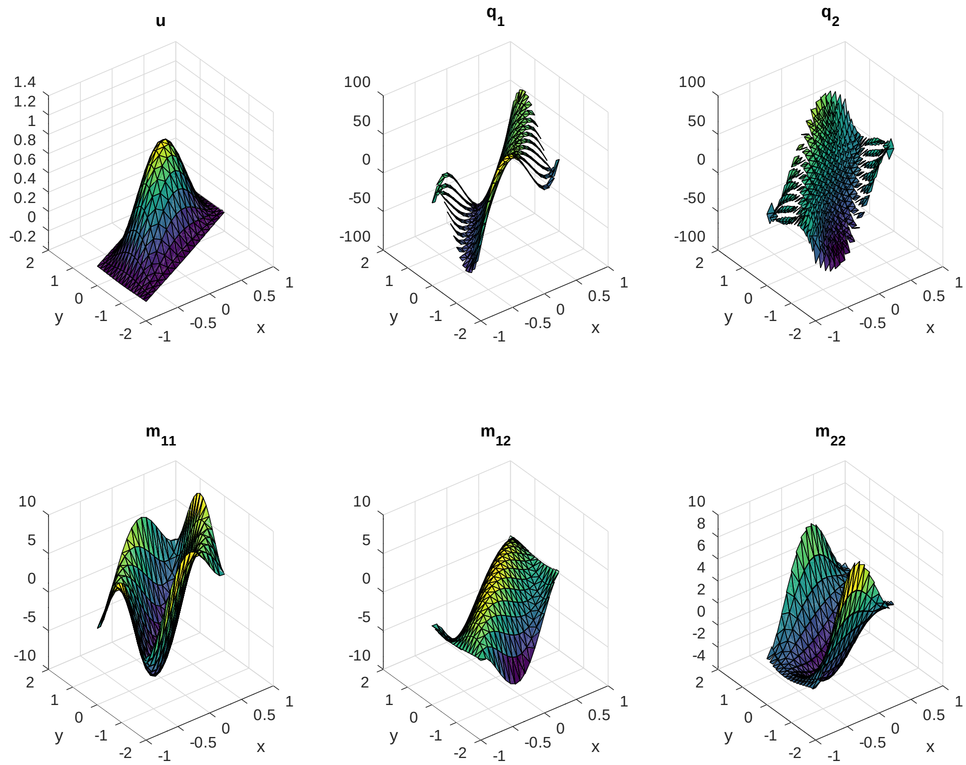

Figure 1: Approximate solution for Example 1 with mesh of 256 elements.

Example 2.

L-shaped domain (figure on the right),
exact solution:

$$u(r,\phi) = r^{1+\alpha}\Big(\cos[(\alpha+1)(\phi-\pi/4)] + C\cos[(\alpha-1)(\phi-\pi/4)]\Big),$$
$$f = \Delta^2 u = 0,\ \alpha \approx 0.54448,\ C \approx 1.8414,\ (r,\phi) \text{ polar coordinates},$$

boundary conditions: $u = \partial_{\boldsymbol{n}} u = 0$ on $(-1,0] \times \{0\} \cup \{0\} \times (-1,0]$,
non-homogeneous Neumann otherwise.

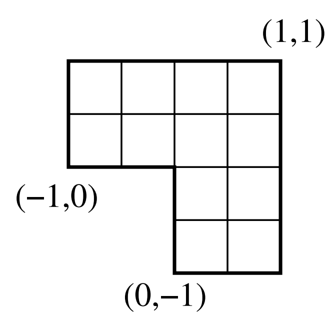

This is a singular case with $\boldsymbol{M} \in \mathbb{H}^{\alpha-\epsilon}(\Omega)\ \forall \epsilon > 0$, that is, $\boldsymbol{M} \notin \mathbb{H}^1(\Omega)$ and with shear force $\mathbf{div}\boldsymbol{M} \notin \boldsymbol{L}_2(\Omega)$. Additionally, we consider mixed boundary conditions, homogeneous Dirichlet data at the edges that touch the origin, and non-homogeneous Neumann data along the other edges. These Neumann traces are given by a restricted version of $\mathrm{tr}^{\mathrm{dDiv}}$ (calculating $\mathrm{tr}_\Omega^{\mathrm{dDiv}}(\boldsymbol{M})$ with test functions $z \in H^2(\Omega)$ that vanish on the Dirichlet edges). Note that Neumann conditions are essential for the mixed scheme. We approximate the Neumann trace by projection onto the corresponding degrees of freedom, and implement the result by using a Lagrange multiplier.

Figures 3 and 4 illustrate the exact solution and approximate solution on a mesh of 192 squares, respectively, in the same format as before (vertical deflection and shear force in the top row, bending moments in the bottom row). The L_2-errors of u and $\boldsymbol{M}$ are plotted in Figure 5, along with curves of orders $O(N^{-\alpha/2}) = O(h^\alpha)$ and $O(N^{-\alpha}) = O(h^{2\alpha})$. The results indicate convergence $\|u - u_h\| = O(h^{2\alpha})$ and $\|\boldsymbol{M} - \boldsymbol{M}\| = O(h^\alpha)$. Although we have not derived any error estimate for singularities, the rate $O(h^\alpha)$ is expected for $\boldsymbol{M} \in \mathbb{H}^{\alpha-\epsilon}(\Omega)$ whereas the results for u indicate super-convergence. We note that $f = \mathrm{div}\mathbf{div}\boldsymbol{M} = 0$ in this example and $\mathrm{div}\mathbf{div}\boldsymbol{M}_h$ is zero up to rounding errors, so that the errors $\|\mathrm{div}\mathbf{div}(\boldsymbol{M} - \boldsymbol{M}_h)\|$ are not plotted.

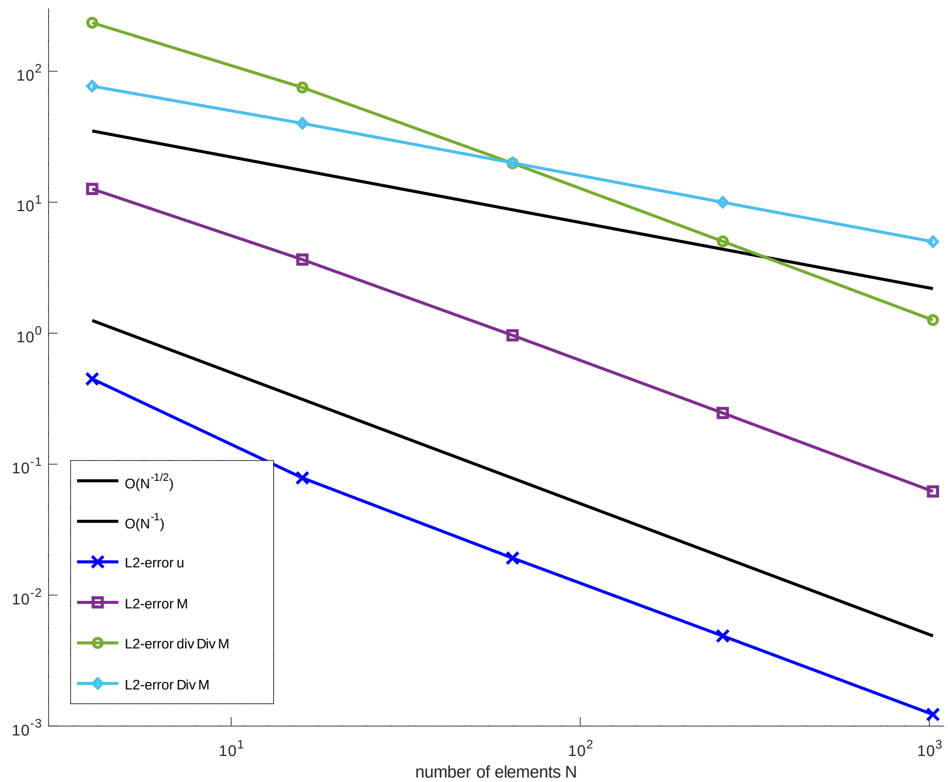

Figure 2: L_2-errors of u, $\boldsymbol{M}$, $\mathrm{div}\,\mathbf{div}\boldsymbol{M}$, and $\boldsymbol{q} = \mathbf{div}\boldsymbol{M}$ for Example 1.

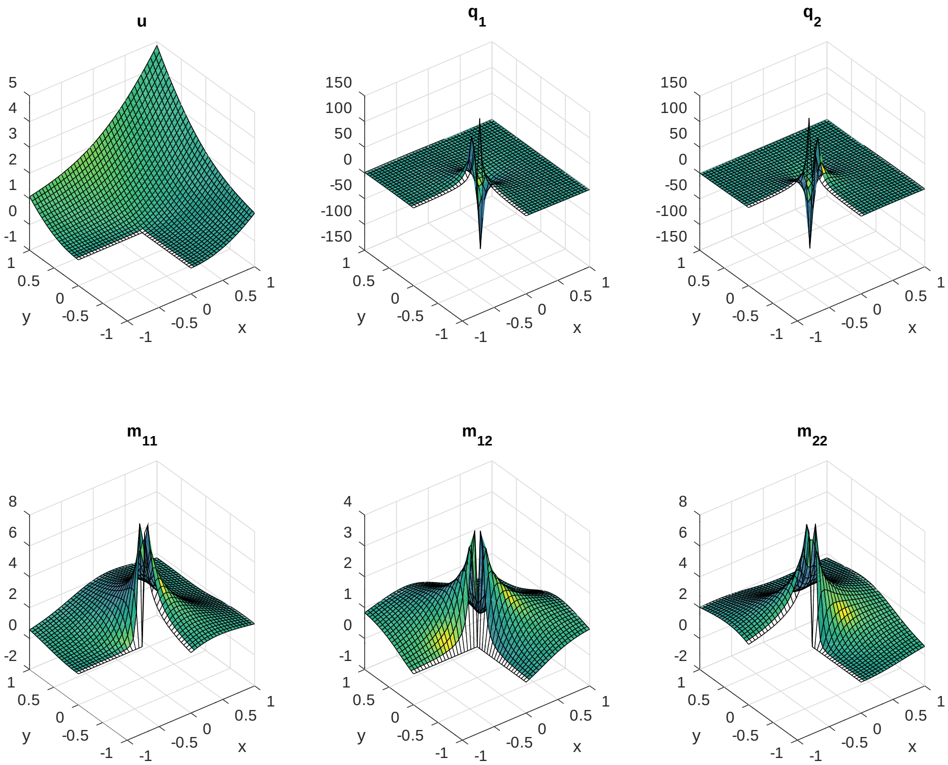

Figure 3: Exact solution for Example 2.

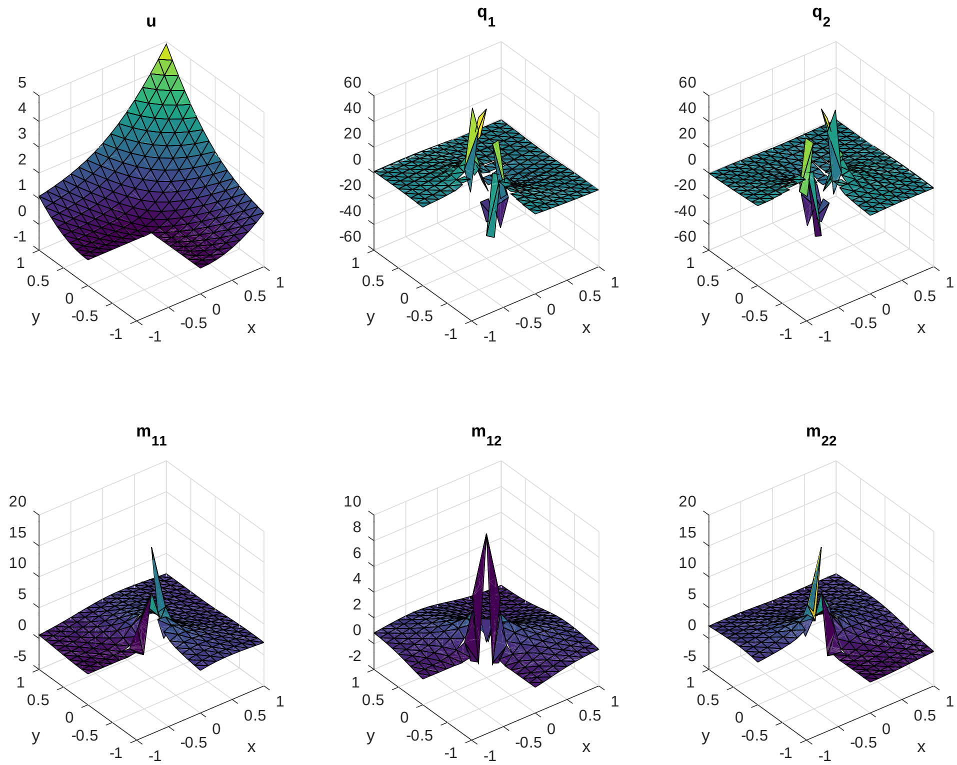

Figure 4: Approximate solution for Example 2 with mesh of 192 elements.

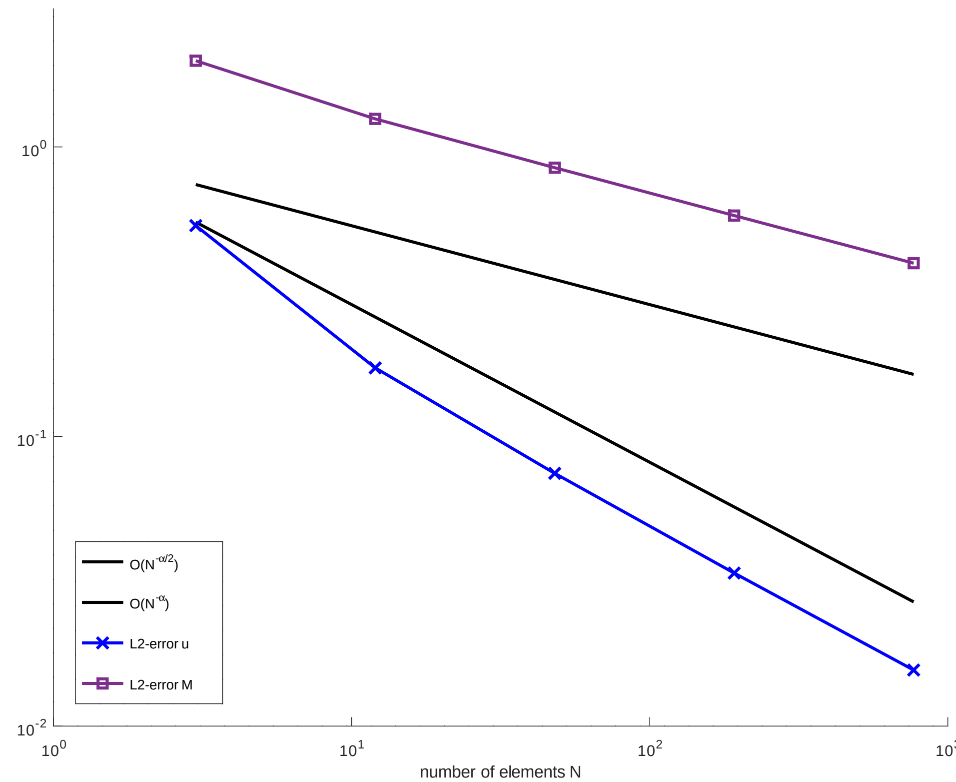

Figure 5: L_2-errors of u and $\boldsymbol{M}$ for Example 2.

A Plots of shape functions

For illustration, we show one reference basis (shape) function from each of the categories of degrees of freedom (4). In every case, the upper row shows the components of the tensor, and the lower row contains the two components of its divergence and the image under operator div**div**. Figure 6 shows $\mathbf{\Phi}_1$ (representing the lowest-order moment of the normal-normal trace on the south edge), Figure 7 shows $\mathbf{\Phi}_5$ (representing the first-order moment of the normal-normal trace on the south edge), Figure 8 shows $\mathbf{\Phi}_9$ (representing the lowest-order moment of the effective shear force on the south edge), and Figure 9 shows $\mathbf{\Phi}_{13}$ (representing a point load at the lower-left corner stemming from the jump of the tangential-normal trace there).

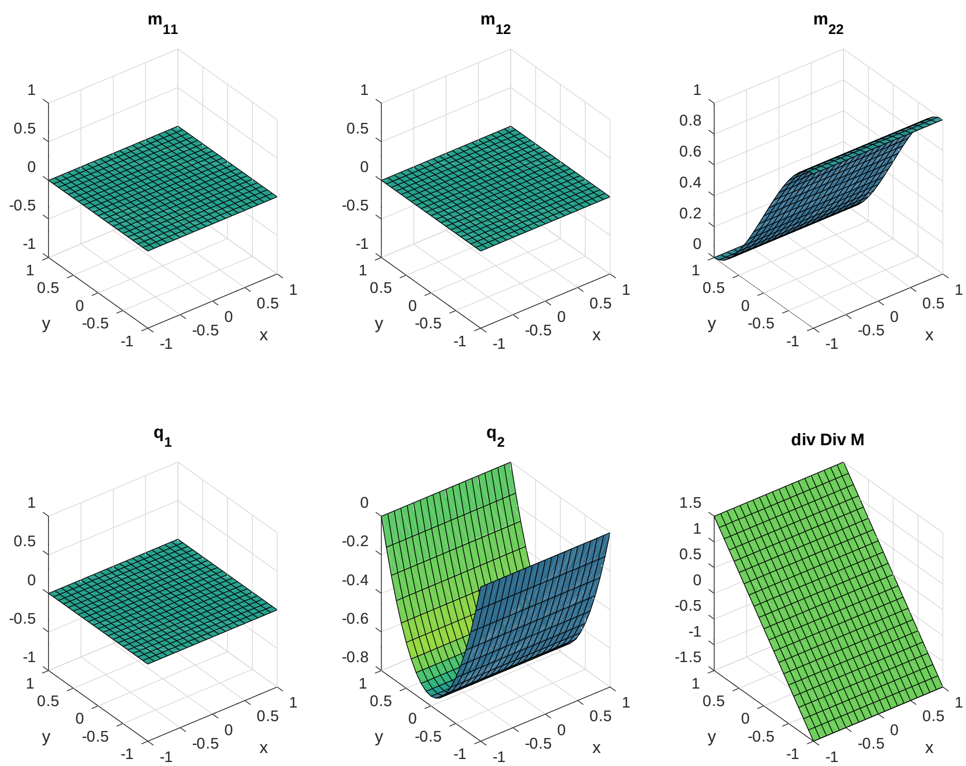

Figure 6: $\boldsymbol{M} = \mathbf{\Phi}_1$ (lowest-order moment of $\boldsymbol{n} \cdot \boldsymbol{M}\boldsymbol{n}$ for edge $(-1, 1) \times \{-1\}$), plots of $\boldsymbol{M}$, $\boldsymbol{q} = \mathbf{div}\boldsymbol{M}$, and $\mathrm{div}\,\mathbf{div}\boldsymbol{M}$.

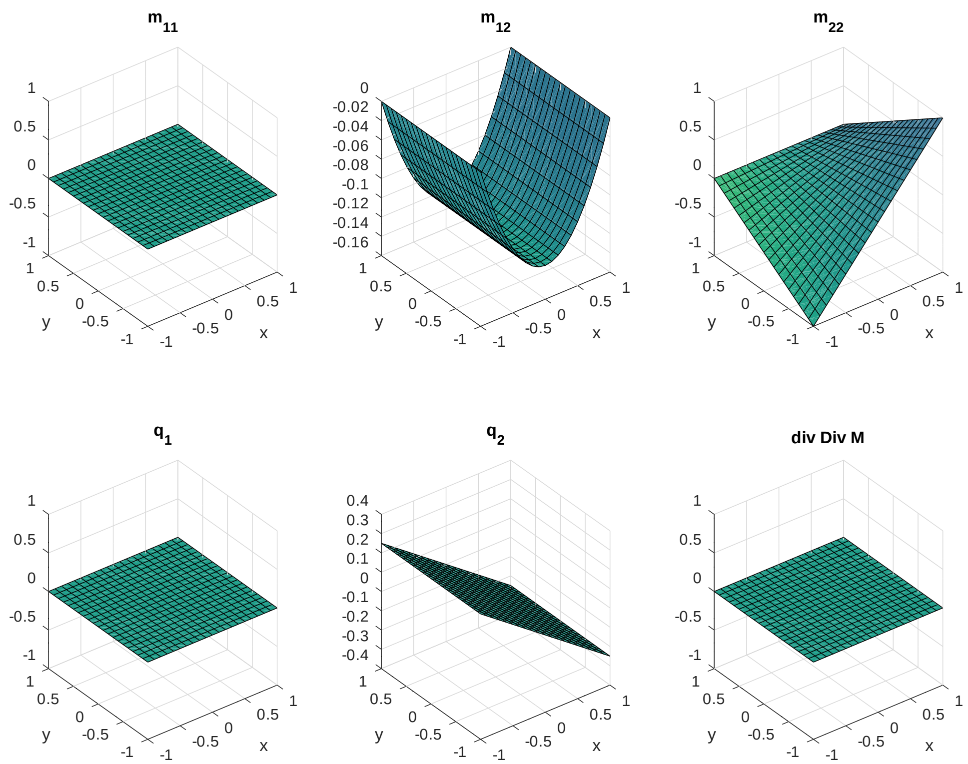

Figure 7: $\boldsymbol{M} = \boldsymbol{\Phi}_5$ (first-order moment of $\boldsymbol{n}\cdot\boldsymbol{M}\boldsymbol{n}$ for edge $(-1,1)\times\{-1\}$), plots of $\boldsymbol{M}$, $\boldsymbol{q} = \mathbf{div}\boldsymbol{M}$, and $\mathrm{div}\mathbf{div}\boldsymbol{M}$.

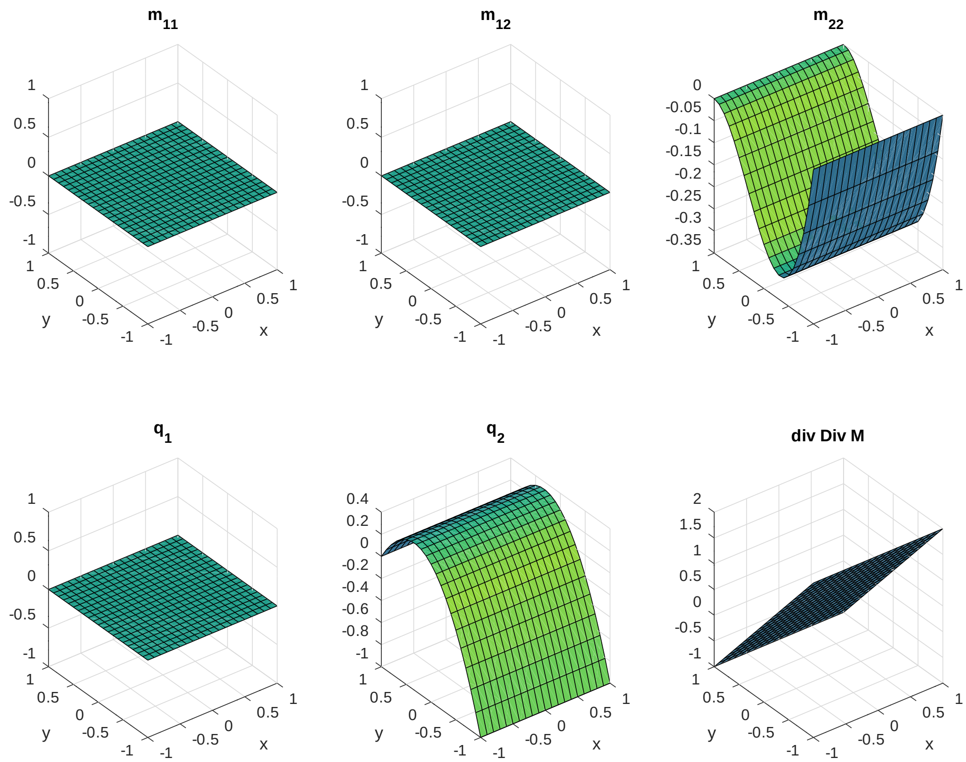

Figure 8: $\boldsymbol{M} = \boldsymbol{\Phi}_9$ (lowest-order moment of effective shear force for edge $(-1,1)\times\{-1\}$), plots of $\boldsymbol{M}$, $\boldsymbol{q} = \mathbf{div}\boldsymbol{M}$, and $\mathrm{div}\mathbf{div}\boldsymbol{M}$.

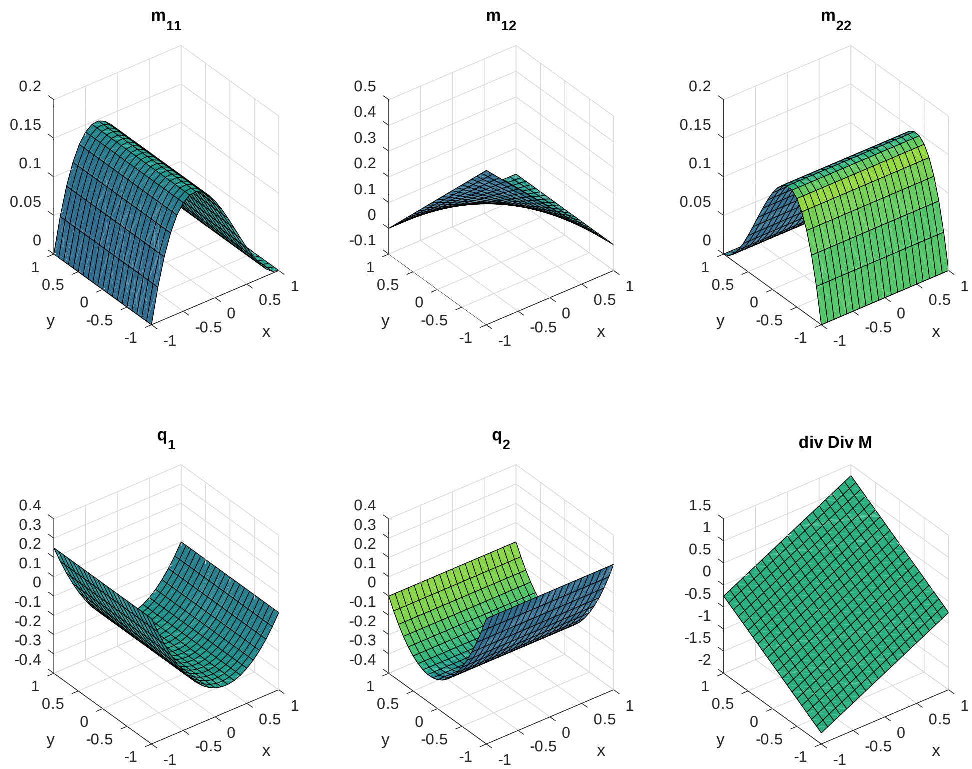

Figure 9: $\boldsymbol{M} = \boldsymbol{\Phi}_{13}$ (jump of $\boldsymbol{t}\cdot\boldsymbol{M}\boldsymbol{n}$ at $(-1,-1)$), plots of $\boldsymbol{M}$, $\boldsymbol{q} = \mathbf{div}\boldsymbol{M}$, and $\mathrm{div}\mathbf{div}\boldsymbol{M}$.

References

[1] R. A. Adams, *Sobolev spaces*, Academic Press, New York-London, 1975. Pure and Applied Mathematics, Vol. 65.

[2] A. Bespalov and N. Heuer, *A new* $\mathbf{H}(\mathrm{div})$*-conforming p-interpolation operator in two dimensions*, ESAIM Math. Model. Numer. Anal., 45 (2011), pp. 255–275.

[3] H. Blum and R. Rannacher, *On the boundary value problem of the biharmonic operator on domains with angular corners*, Math. Methods Appl. Sci., 2 (1980), pp. 556–581.

[4] D. Boffi, F. Brezzi, and M. Fortin, *Mixed finite element methods and applications*, vol. 44 of Springer Series in Computational Mathematics, Springer, Heidelberg, 2013.

[5] J. H. Bramble and R. S. Falk, *Two mixed finite element methods for the simply supported plate problem*, RAIRO Anal. Numér., 17 (1983), pp. 337–384.

[6] L. Chen and X. Huang, *Finite elements for* $\mathrm{div}\,\mathrm{div}$*-conforming symmetric tensors*, arXiv:2005.01271, 2021.

[7] ——, *Finite elements for* $\mathrm{div}\,\mathrm{div}$ *conforming symmetric tensors in three dimensions*, Math. Comp., 91 (2022), pp. 1107–1142.

[8] P. G. Ciarlet and P.-A. Raviart, *A mixed finite element method for the biharmonic equation*, Math. Res. Center, Univ. of Wisconsin-Madison, Academic Press, New York, 1974, pp. 125–145. Publication No. 33.

[9] R. S. Falk, *Approximation of the biharmonic equation by a mixed finite element method*, SIAM J. Numer. Anal., 15 (1978), pp. 556–567.

[10] T. Führer, A. Haberl, and N. Heuer, *Trace operators of the bi-Laplacian and applications*, IMA J. Numer. Anal., 41 (2021), pp. 1031–1055.

[11] T. Führer and N. Heuer, *Fully discrete DPG methods for the Kirchhoff–Love plate bending model*, Comput. Methods Appl. Mech. Engrg., 343 (2019), pp. 550–571.

[12] T. Führer, N. Heuer, and A. H. Niemi, *An ultraweak formulation of the Kirchhoff–Love plate bending model and DPG approximation*, Math. Comp., 88 (2019), pp. 1587–1619.

[13] G. N. Gatica, *A simple introduction to the mixed finite element method*, SpringerBriefs in Mathematics, Springer, Cham, 2014. Theory and applications.

[14] K. Hellan, *Analysis of elastic plates in flexure by a simplified finite element method*, Acta Polytech. Scand. Civ. Eng. Build. Constr. Ser. 46, 1 (1967).

[15] L. R. Herrmann, *Finite-element bending analysis for plates*, J. Eng. Mech. Div., 93 (1967), pp. 13–26.

[16] N. Heuer, *On the equivalence of fractional-order Sobolev semi-norms*, J. Math. Anal. Appl., 417 (2014), pp. 505–518.

[17] J. Hu, R. Ma, and M. Zhang, *A family of mixed finite elements for the biharmonic equations on triangular and tetrahedral grids*, Sci. China Math., 64 (2021), pp. 2793–2816.

[18] C. Johnson, *On the convergence of a mixed finite-element method for plate bending problems*, Numer. Math., 21 (1973), pp. 43–62.

[19] W. McLean, *Strongly Elliptic Systems and Boundary Integral Equations*, Cambridge University Press, 2000.

[20] P. Monk, *A mixed finite element method for the biharmonic equation*, SIAM J. Numer. Anal., 24 (1987), pp. 737–749.

[21] A. Pechstein and J. Schöberl, *Tangential-displacement and normal-normal-stress continuous mixed finite elements for elasticity*, Math. Models Methods Appl. Sci., 21 (2011), pp. 1761–1782.